PAPER

Statistical validation of predictive TRANSP simulations of baseline discharges in preparation for extrapolation to JET D–T

IOP Publishing | International Atomic Energy Agency Nuclear Fusion

Nucl. Fusion **57** (2017) 066032 (8pp) https://doi.org/10.1088/1741-4326/aa6b80

Statistical validation of predictive TRANSP simulations of baseline discharges in preparation for extrapolation to JET D–T

Hyun-Tae Kim[1,2], M. Romanelli[2], X. Yuan[3], S. Kaye[3], A.C.C. Sips[4], L. Frassinetti[5], J. Buchanan[2] and JET Contributors[6,a]

[1] EUROfusion PMU, Culham Science Centre, Abingdon, OX14 3DB, United Kingdom
[2] Culham Centre for Fusion Energy, Culham Science Centre, Abingdon, OX14 3DB, United Kingdom
[3] Princeton Plasma Physics Laboratory, Princeton University, Princeton, NJ 08543, United States of America
[4] JET Exploitation Unit, Culham Science Centre, Abingdon OX14 3DB, United Kingdom
[5] Division of Fusion Plasma Physics, KTH Royal Institute of Technology, SE-10691 Stockholm, Sweden
[6] EUROfusion Consortium, JET, Culham Science Centre, Abingdon, Ox14 3DB, United Kingdom

E-mail: hyun-tae.kim@euro-fusion.org

Received 7 December 2016, revised 16 March 2017
Accepted for publication 5 April 2017
Published 3 May 2017

Abstract

This paper presents for the first time a statistical validation of predictive TRANSP simulations of plasma temperature using two transport models, GLF23 and TGLF, over a database of 80 baseline H-mode discharges in JET-ILW. While the accuracy of the predicted T_e with TRANSP-GLF23 is affected by plasma collisionality, the dependency of predictions on collisionality is less significant when using TRANSP-TGLF, indicating that the latter model has a broader applicability across plasma regimes. TRANSP-TGLF also shows a good matching of predicted T_i with experimental measurements allowing for a more accurate prediction of the neutron yields. The impact of input data and assumptions prescribed in the simulations are also investigated in this paper. The statistical validation and the assessment of uncertainty level in predictive TRANSP simulations for JET-ILW-DD will constitute the basis for the extrapolation to JET-ILW-DT experiments.

Keywords: TRANSP, TGLF, GLF23, DT campaign, JET

(Some figures may appear in colour only in the online journal)

Introduction

The EUROfusion Consortium is planning deuterium–tritium (D–T) experimental campaigns in 2019 in JET with the ITER-like wall (ILW) to address physics issues which are important for ITER D–T experiments [1]. To achieve the scientific objectives, JET operation should demonstrate 10–15 MW of fusion power for at least 5 s, a performance never attempted before in fusion research history. Previously, JET and TFTR produced a peak fusion power of 16.1 MW in 1997 [2] and 10.7 MW in 1994 [3] respectively, but steady state operation with such a high fusion power has never been achieved. In order to prepare these unprecedented JET operational scenarios with D–T mixtures, reliable predictive simulations are of crucial importance. However, the current capability to predict plasma temperature evolution and the resultant fusion power is still limited. This is mainly due to the incompleteness of turbulent transport models and the uncertainties of the input data (e.g. pedestal top temperature, radiation, rotation profiles, etc). In addition to these issues limiting the present prediction capability, the D–T mixture would add even further uncertainties resulting from hydrogenic isotopes and alpha particles physics. Quantification of the impact of the foreseen uncertainties on reproducing the present discharges has therefore a high priority in preparation for the extrapolation to JET D–T experiments. In this paper, the current prediction capability of T_e, T_i, and neutron yields

[a] See the author list of 'Overview of the JET results in support to ITER' by X. Litaudon *et al* to be published in *Nuclear Fusion* Special issue: overview and summary reports from the *26th Fusion Energy Conf. (Kyoto, Japan, 17–22 October 2016)*.

with predictive TRANSP [4, 5] simulations where the turbulent transport is calculated by GLF23 [6, 7] and TGLF [8, 9] is assessed statistically over 80 baseline H-mode discharges at JET-ILW. In order to take into account the uncertainties due to the input data and assumptions, all discharges were simulated using identical default simulation settings. Based on these reference simulations, the impact of collisionality regime, pedestal top temperature, radiation profile, and toroidal rotation on temperature profile predictions are investigated by modifying an input or an assumption in the reference simulation settings. The above statistical validation of predictive TRANSP simulations at JET-ILW-DD will constitute the basis for the extrapolation to JET-ILW-DT experiments.

The database of the baseline discharges and the inputs and assumptions used for the reference simulations are introduced in section 1. In section 2, the T_e prediction capability of TRANSP-GLF23 or TRANSP-TGLF are assessed via a comparison with the T_e measured by high resolution Thomson scattering (HRTS) [10], and the impacts of the input data and assumptions used on the T_e predictions are investigated. In section 3, the T_i prediction capability is also assessed by comparison with the T_i measured by charge exchange (CX) spectroscopy [11]. In section 4, the impact of the predicted T_i on the resultant neutron yield calculation is investigated by comparing the calculated neutron yields to the neutron yields measured by fission chamber [12, 13]. The conclusion of the paper is provided in section 5.

1. Input and assumptions

The database consists of 80 baseline H-mode discharges with JET-ILW which cover a large range of the engineering parameters as well as the dimensionless plasma parameters.

- 46 discharges selected for ITPA database [14]: low q_{95}(=2.7–3.3) experiments for 2012–2014, stationary state for 5 confinement times (τ_E) in baseline H-mode (i.e. $\beta_N > 0.85$ β_N, max), rotation profile available, I_p (=2–3.5 MA), B_t (=1.9–3.2 T), P_{heat} (=10.8–27.7 MW), T_{e0} (=2.2–6 keV), $\langle n_e \rangle$ (=4–10.2 $\times$ 10^{19} m^{-3}), β_N (=1–2)
- 22 discharges selected for dimensionless plasma parameter scanning [15]: $\nu^* = 0.04$–0.15 at ($\rho = 0.4$), $\rho^* = 0.003$–0.005
- 10 discharges selected for comparative confinement study [16]: I_p (=2.5 MA), B_t (=2.7 T), P_{heat} (=14–17 MW), $\langle n_e \rangle$ (=7.1–10.2 $\times$ 10^{19} m^{-3})
- 2 reference discharges selected for the task of DT scenario extrapolation at JET (called T15-01) i.e. 87215 and 87412

For the 80 reference predictive simulations, core temperatures T_e and T_i are predicted over the radial regions $\rho = 0$–0.9, and the boundary condition for temperature profile computation was given by experimental data at $\rho = 0.9$. The input settings and assumptions used in the reference simulations are the following:

- T_e boundary condition is prescribed by the experimental measurement of HRTS at $\rho = 0.9$
- T_i boundary condition is assumed to have $T_i = T_e$ at $\rho = 0.9$
- Whole profile of electron density n_e (i.e. $\rho = 0$–1) is prescribed by experimental measurement of HRTS [10]
- Turbulent transport for $\rho = 0$–0.9 is computed by GLF23 [6, 7] or TGLF [8, 9]
- Neoclassical transport for $\rho = 0$–0.9 is computed by NCLASS [17]
- Uniform radiation profile is prescribed by bolometry measurement (i.e. BOLO/TOBU) [18]
- Uniform Zeff profile is prescribed by bremsstrahlung [19] assuming Be is the only impurity.
- Toroidal rotation profile is prescribed by the measurement of CX spectroscopy [11]
- Heating and particle source terms calculated consistently by NUBEAM [5, 20] and TORIC [21, 22]

2. Prediction of the electron temperature

In this section, the impacts of collisionality regime with different turbulent transport solver (i.e. GLF23 or TGLF), T_e boundary condition, radiation profile input, and toroidal rotation prediction on predicting T_e in TRANSP were individually investigated by modifying only one simulation setting from the reference settings defined in section 1.

2.1. Impact of collisionality regime

The current T_e prediction capability with TRANSP-GLF23 for baseline H-mode JET-ILW discharges is presented in figure 1(*a*) where the predicted T_e values are compared to the T_e measured by HRTS. Each symbol indicates T_e averaged over different radial windows i.e. black circles ($\rho = 0.3$–0.5), red diamonds ($\rho = 0.5$–0.7), and blue squares ($\rho = 0.7$–0.9). As the line of sight of HRTS measurement in the discharges is deviated from the magnetic axis, T_e data for $\rho = 0$–0.3 is not available to compare in figure 1(*a*). Overall, TRANSP-GLF23 simulations reproduce T_e with a Pearson correlation coefficient[7] of 0.714 [23]. From the edge region to the core region (i.e. blue squares, red diamonds, and black circles in order), the predicted T_e becomes more deviated from the HRTS measurement, as the boundary condition of T_e is given by the T_e measured at $\rho = 0.9$. Furthermore, a number of the predicted core T_e ($\rho = 0.3$–0.5) are under-predicted, as indicated by the green dashed ellipse in figure 1(*a*). These discharges have low core collisionality ν^*(<0.08) in common, and figure 1(*b*) shows more clearly that the core T_e reproducibility with TRANSP-GLF23 is subject to core ν^* i.e. under-prediction at low core ν^* and over-prediction at high core ν^*.

The same analysis has been done with 'Trapped' GLF (TGLF), which is a more complete turbulent transport model solving gyro-Landau-fluid (GLF) equations [24] with better accuracy than GLF23 [25]. While GLF23 solves an 8 $\times$ 8 matrix eigenvalue problem i.e. 4 moments equations with

[7] Pearson correlation coefficient is defined as $\frac{\mathrm{cov}(X,Y)}{\sigma_X \sigma_Y}$ where cov(X, Y) is the covariance, and σ_X and σ_Y are the standard deviation of X and Y, respectively.

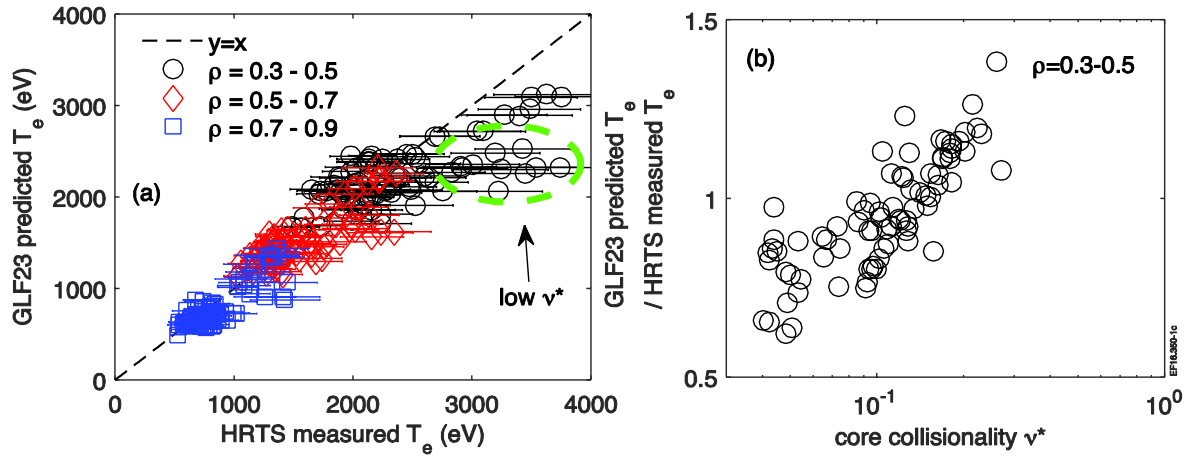

Figure 1. (*a*) T_e predicted by TRANSP-GLF23 using the reference simulation settings is compared to T_e measured by HRTS. The comparison is made over 80 baseline H-mode JET-ILW discharges. The radial windows in which T_e is averaged are indicated by blue squares ($\rho = 0.7$–0.9), red diamonds ($\rho = 0.5$–0.7), and black circles ($\rho = 0.3$–0.5). T_e predicted by TRANSP-GLF23 shows a Pearson correlation coefficient of 0.714. (*b*) The impact of ν^* on the ratio of the predicted T_e to the measured T_e is shown. T_e and core ν^* are averaged over $\rho = 0.3$–0.5.

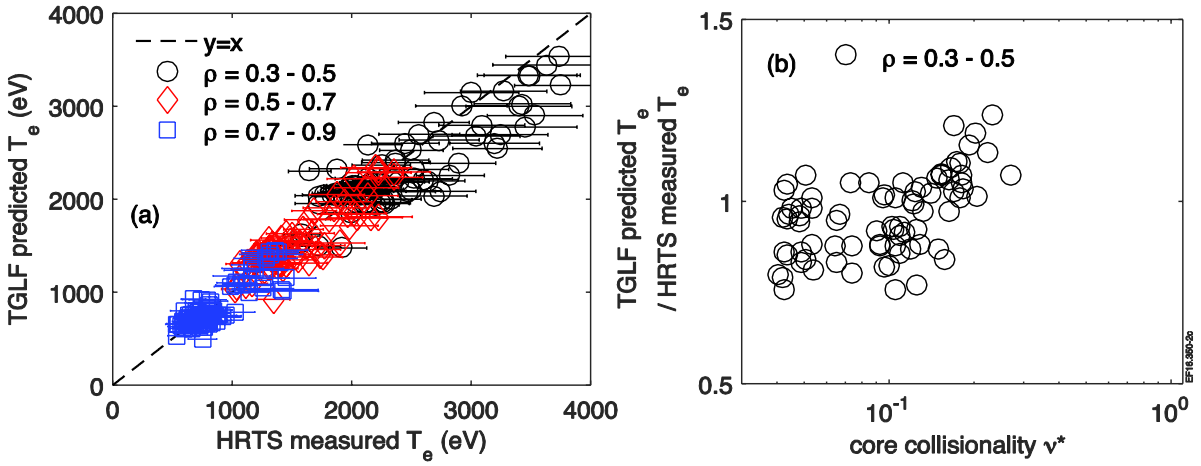

Figure 2. (*a*) and (*b*) T_e is predicted by TRANSP-TGLF. Otherwise, it is the same analysis as in figures 1(*a*) and (*b*). T_e predicted by TRANSP-TGLF has a Pearson correlation coefficient of 0.869.

2 species +1 poloidal basis function, TGLF solves a 120 × 120 matrix eigenvalue problem i.e. 15 moments (12 for passing particles and 3 for trapped particles) with 2 species +4 poloidal basis functions [9]. This enables modelling of trapped particles in a more complete way in TGLF. While a more completed approach for this should be possible with gyrokinetic simulations, the computation of transport with gyrokinetic simulations for a large radial region is too expensive for routine use. Although TGLF is also computationally much more expensive than GLF23, it is still affordable to routinely perform simulations for a large radial region i.e. $\rho = 0$ ~ pedestal top, together with a consistent source calculations of heat and particles from NBI and ICRH. The consequence of the main improvement in TGLF is indeed shown in figure 2(*a*). The T_e predicted by TRANSP-TGLF shows better agreement with the measured T_e having a Pearson correlation coefficient of 0.869, and the under-prediction of the core T_e at low core ν^* is much less significant (see figure 2(*b*)).

The dependencies of core T_e prediction (i.e. for $\rho = 0.3$–0.5) on core ν^* in TRANSP-GLF23 and TRANSP-TGLF are compared with the discharges selected for ν^* scan where the other dimensionless parameters (i.e. $\rho*$ and β_N) are maintained. Figure 3(*a*) clearly shows that the under-prediction of T_e at low core ν^* is much less significant in TRANSP-TGLF than in TRANSP-GLF23.

Recalling that ν^* is the ratio of the effective collision frequency for trapped particles to the frequency of their bounce orbit,

$$\nu_e^* \equiv \frac{\nu_e}{\text{freq of the bounce orbit}} = \frac{\nu_e R q}{(R/q)^{3/2}(kT_e/m_e)^{0.5}}$$

$$\text{where } \nu_e = \frac{2.91\,\text{e}-12 \times n_e \ln\Lambda}{T_e^{3/2}(\text{eV})},$$

the likelihood of a particle completing a bounce orbit increases in the low ν^* regime, and the model of trapped particle physics therefore becomes important. The under-prediction of T_e at

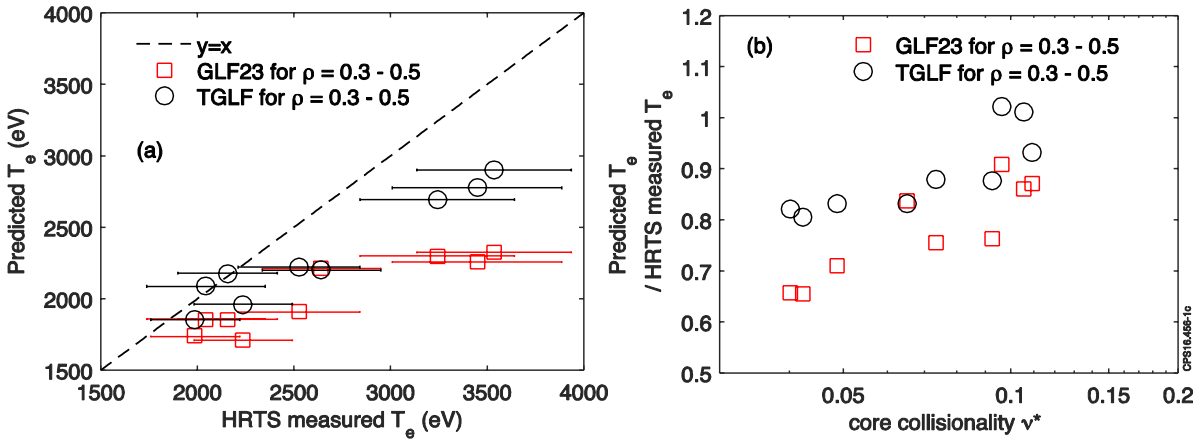

Figure 3. (*a*) Comparison of T_e predicted with TRANSP-GLF23 (red squares) and TRANSP-TGLF (black circles) over the discharges of ν^* scan database where the other dimensionless parameters do not vary. (*b*) The impact of core ν^* on core T_e prediction in TRANSP-GLF23 and TRANSP-TGLF is shown. T_e and core ν^* are averaged over $\rho = 0.3$–0.5.

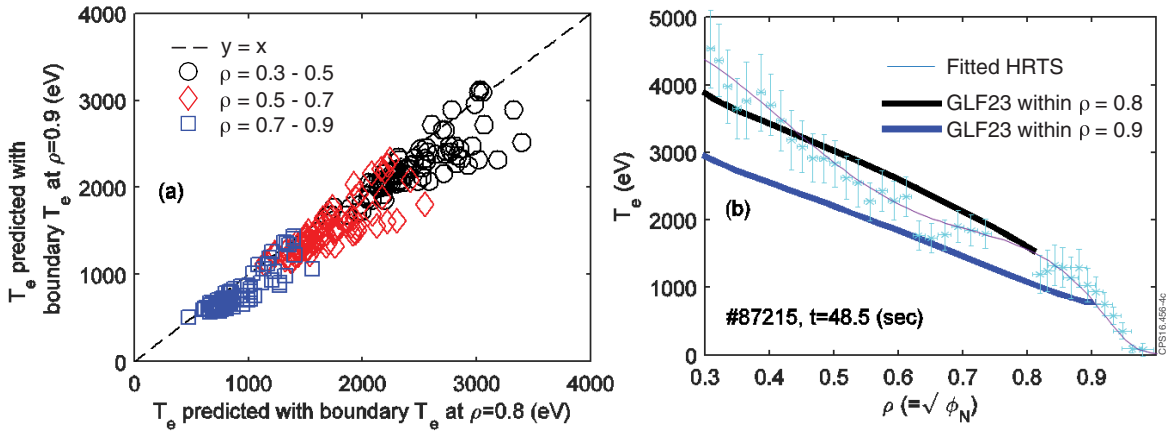

Figure 4. (*a*) The impact of the T_e boundary position on T_e prediction with TRANSP-GLF23 is shown. The notation of the symbols are the same as figure 1(*a*). (*b*) One of the typical discharges where the ETB region is wider than $\rho = 0.9$–1 is shown. The T_e profiles predicted with GLF23 using the T_e boundary condition given at $\rho = 0.9$ (blue) or $\rho = 0.8$ (black) are compared. The experimental data of HRTS measurement with error bars and the fitted profile are also shown.

low ν^* implies that the turbulent heat fluxes associated with the trapped particles are over-calculated. Figure 3(*b*) shows that when the other dimensionless parameters are maintained the dependency of T_e prediction on ν^* is more visible, and under-calculation of T_e is more significant in GLF23 where the trapped particle model is more simplified than TGLF.

2.2. Impact of T_e boundary condition

Neither GLF23 nor TGLF includes the transport in the edge transport barrier (ETB), and the steeper T_e profile in the ETB region is therefore not calculated correctly using the present core turbulent transport models. This requires the pedestal top T_e as a boundary condition. For present discharges a correct pedestal top T_e can be found from measurements, but for future discharges it requires assumptions. The impact of T_e boundary condition on core T_e prediction therefore needs to be investigated. For this investigation, the T_e boundary condition in the simulations is given by the fitted HRTS profiles at $\rho = 0.8$, and the temperature predictions are made for $\rho = 0$–0.8. In figure 4(*a*), the TRANSP-GLF23 predictive simulation results with this modified setting are compared against the reference simulations where the T_e boundary position was $\rho = 0.9$. Note, the inputs and assumptions in these two simulation groups are identical, apart from the T_e boundary position. Figure 4(*a*) shows that in some discharges the predicted values of core T_e are increased by setting the boundary T_e at $\rho = 0.8$. This is due to the fact that in those discharges the width of the ETB region is wider than $\rho = 0.9$–1. One of the typical discharges with such a wide ETB region is shown in figure 4(*b*) where the T_e profile measured by the HRTS and the T_e profiles predicted with different T_e boundary position are compared. As the radial position $\rho = 0.9$ of the T_e boundary condition is not inner enough to exclude the ETB region, the steep gradient of the T_e profile in the ETB region is not reproduced in the simulations. As a result, the T_e predicted at $\rho = 0.8$ with the T_e boundary condition given at $\rho = 0.9$ is lower than the measured T_e at $\rho = 0.8$, and the predicted core T_e with the T_e boundary condition at $\rho = 0.9$ is thus also lower than that with the T_e boundary condition given at $\rho = 0.8$. However, it is worth noting that the gradient of the core T_e profile is not significantly modified by different T_e boundary conditions. Although it is not shown

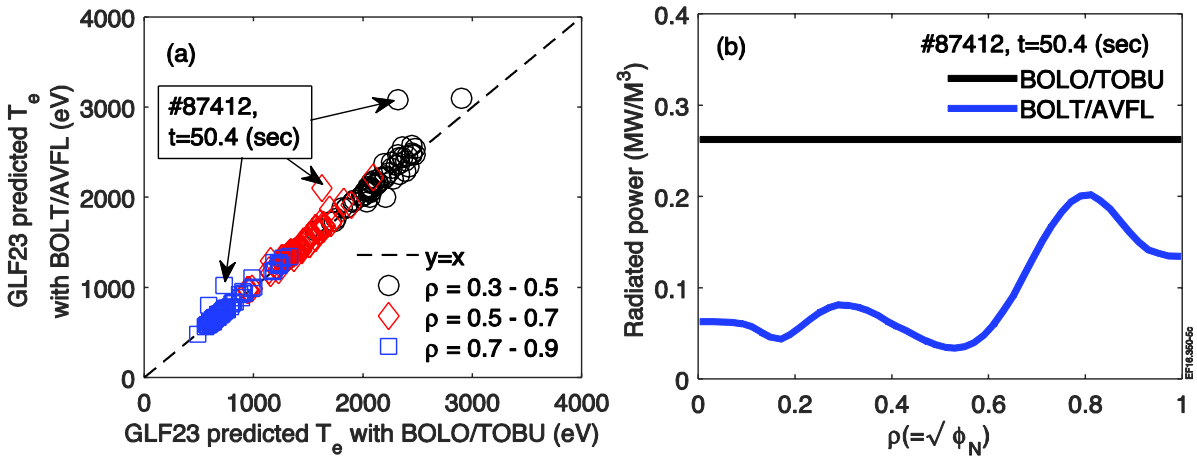

Figure 5. (*a*) The impact of the radiation profile on T_e prediction with TRANSP-GLF2. The notation of the symbols is the same as figure 1(*a*). (*b*) Uniform radiated power (BOLO/TOBU) and radiation profile (BOLT/AVFL) in #87412 are compared.

in this paper, the same feature is also observed in TRANSP-TGLF. This feature implies that the predicted core T_e can be changed by different assumptions of T_e boundary condition, but not more than the difference in the assumed boundary T_e.

2.3. Impact of radiation profile

In the bolometry measurement system at JET, the total radiated power is automatically produced by inter-shot analysis. While the total radiated power can be used as an input data in predictive simulations assuming a uniform radiation profile, there was a concern about the profile effects of radiated power on T_e prediction. However, as there is no automatic routine available to reconstruct radiation profiles, the radiation profile data can only be produced manually, requiring considerable human effort. This is not desirable to build a large database of predictive simulations. The impact of radiation profile is assessed by comparing 80 TRANSP-GLF23 simulations with reconstructed radiation profiles to the reference simulations with the default setting (i.e. with uniform radiation). As shown in figure 5(*a*), for a vast majority of predictive simulations, the impact of the profiles of radiated power is negligible. The impact is only visible in discharge #87412, but it turned out that in this discharge the total radiated power differs significantly between uniform radiation and radiation profile (see figure 5(*b*)). Hence, the profile effect of radiated power is not important for the predictive simulations of JET-ILW baseline discharges, as long as the estimate of the total radiated power is correct. This enables one to assume only total radiation power when predicting future discharges, rather than having to assume a more complicated radiation profile.

2.4. Impact of toroidal rotation frequency

The toroidal rotation frequency has an impact on predicting temperature profiles as it determines the *ExB* flow shear stabilisation of turbulent heat flux. In GLF23, the turbulence quench rule, $\gamma_{net} = \gamma_{max} - \alpha_E \gamma_{E\times B}$, is adopted [7] where γ_{max} is the maximum growth rate of the drift-wave instabilities, and $\gamma_{E\times B}$ $(=(r/q)\mathrm{d}(qV_{E\times B}/r)/\mathrm{d}r)$ is $E \times B$ flow shearing rate. α_E is a coefficient to adjust the level of $E \times B$ flow shear stabilisation. In this paper, a fixed value of $\alpha_E = 1$ is used for all simulations. In TRANSP-GLF23, the poloidal $E \times B$ flow velocity $V_{E\times B}$ is calculated by $V_{E\times B} = E_r/B_t$ where E_r is a radial electric field and B_t is a toroidal magnetic field. The E_r is calculated by using a zero'th order formula derived from an assumed force balance between the electrostatic force due to E_r and the Lorentz force (i.e. $E_r = V_t B_p$) [26], and here V_t is given by the toroidal rotation frequency. The toroidal rotation frequency can be obtained by analysing CX spectroscopy or by solving the internal momentum transport equation in TRANSP-GLF23 or TRANSP-TGLF. The impact of the toroidal rotation predicted by TRANSP-GLF23 on T_e prediction is shown in figure 6(*a*) by comparing the simulation results against the reference simulations where the rotation frequency was given by CX spectroscopy. Note, in this comparison, the only difference in simulation setting between the two simulation groups is the toroidal rotation i.e. predicted rotation frequency or measured rotation frequency. In a majority of discharges, the T_e predicted with predicted rotation frequency is calculated to be higher than that with measured rotation frequency. As shown by the comparison between the measured rotation and the predicted rotation in figure 6(*b*), this is because TRANSP-GLF23 significantly over-predicts the rotation frequency compared to the CX-measured value, thereby resulting in the excessive $E \times B$ flow shear stabilisation. This indicates that, for predicting future JET-ILW baseline discharges, reasonable assumption of toroidal rotation will be necessary as the rotation prediction is not reliable for the current version of TRANSP-GLF23. The comparison with TRANSP-TGLF simulation results couldn't be made due to the limitation of CPU available, resulting from the expensive computation cost of TGLF.

3. Prediction of the ion temperature

T_i predicted by TRANSP- GLF23 or TRANSP-TGLF over the 80 baseline H-mode discharges are compared against T_i measured by CX spectroscopy in figures 7(*a*) and (*b*), respectively. The comparison of core T_i is limited up to $\rho = 0.4$–1 as the CX data is not available. This is because CX spectroscopy

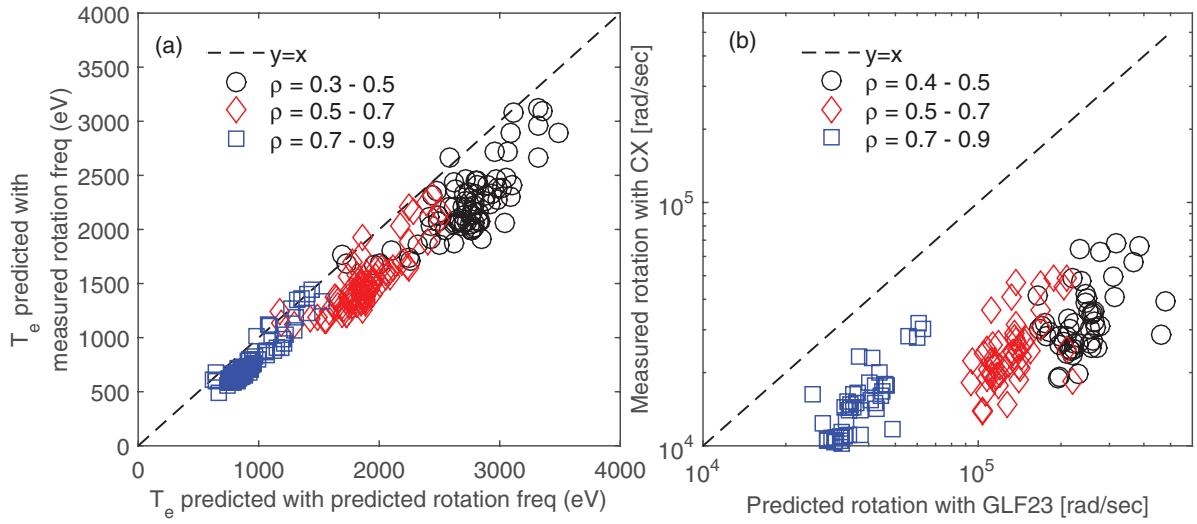

Figure 6. (*a*) The impact of predicted rotation frequency on T_e prediction with TRANSP-GLF23. (*b*) Comparison of toroidal rotation between CX measurement and TRANSP-GLF23 prediction.

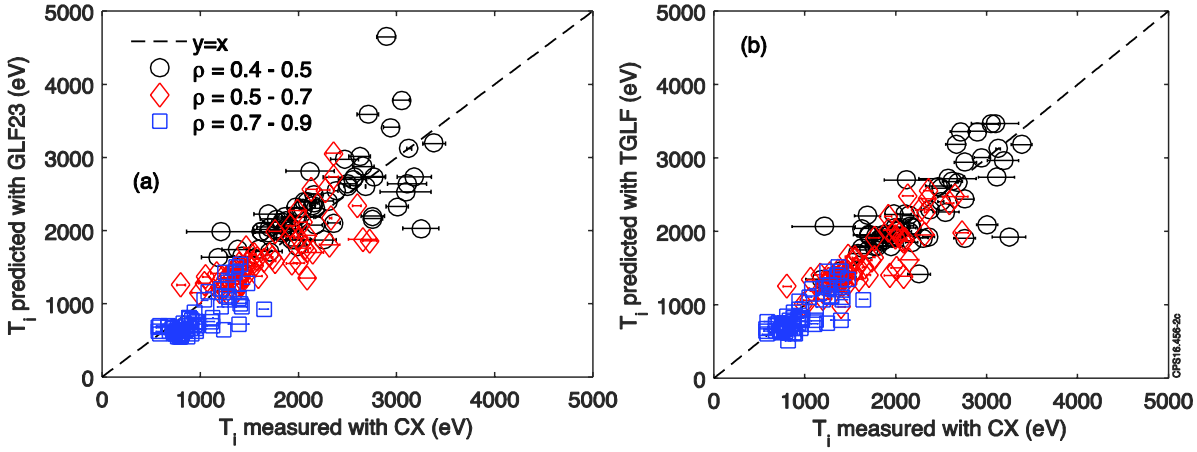

Figure 7. (*a*) T_i predicted by TRANSP-GLF23, i.e. the reference simulations, is compared against T_i measured by CX (Pearson correlation coefficient = 0.696). (*b*) T_i prediction with TRANSP-TGLF is compared against T_i measured by CX (Pearson correlation coefficient = 0.801).

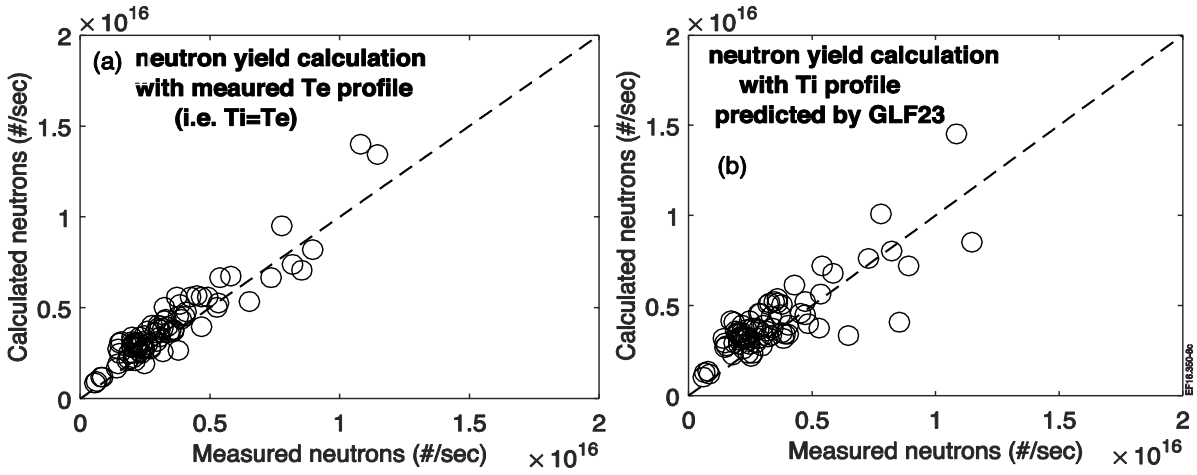

Figure 8. (*a*) In the 80 baseline H-mode discharges, the neutron yields calculated by interpretive TRANSP analysis with HRTS T_e profiles assuming $T_i = T_e$ are compared to the neutron yields measured by the fission chamber. (Pearson correlation coefficient = 0.942). (*b*) The neutron yields are calculated with T_e and T_i predicted by TRANSP-GLF23 i.e. the reference predictive simulations (Pearson correlation coefficient = 0.825).

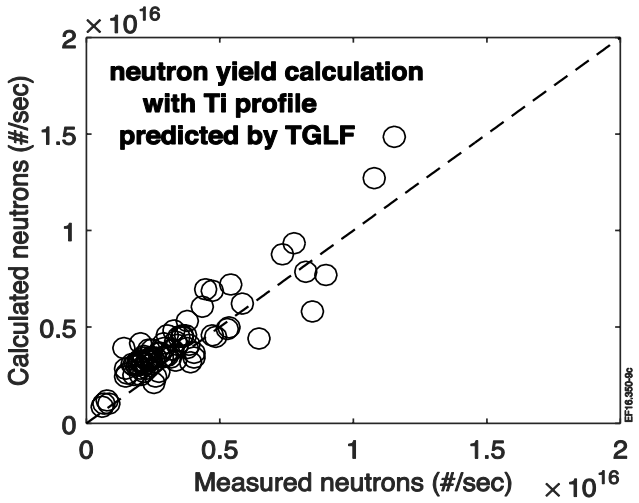

Figure 9. The neutron yields are calculated with T_e and T_i predicted by TRANSP-TGLF. (Pearson correlation coefficient = 0.910.)

analysis has been difficult due to the issue of weak signal since the replacement of the plasma facing components to ILW i.e. Be and W. While a significant uncertainty level of T_i prediction with TRANSP-GLF23 is observed (Pearson correlation coefficient = 0.696), T_i prediction with TRANSP-TGLF has a better accuracy (Pearson correlation coefficient = 0.801). It should be noted that in both GLF23 and TGLF simulations the reproduced T_i include the uncertainty of the T_i boundary condition as it is given at $\rho = 0.9$ assuming $T_i = T_e$ for all the predictive simulations. As discussed before, for some discharges this boundary position is not enough to exclude the ETB layer. The number of discharges with under-predicted T_i would be reduced if the T_i boundary position was shifted into the core e.g. $\rho = 0.8$.

4. Prediction of the neutron yields

The level of T_i prediction accuracy affects neutron yield calculation as the fusion cross-section is a strong function of T_i. Figure 8(*a*) compares the neutron yields calculated by interpretive TRANSP analysis using the HRTS-measured T_e profiles against the neutron yields measured by the fission chamber [12], which was calibrated in 2013 [13]. Here, $T_i = T_e$ is assumed as CX-measured T_i is not available within $\rho < 0.4$. This assumption can be justified as all discharges in this paper are baseline H-mode discharges where the equilibration between electrons and ions is high due to high n_e. As can be seen by the formula for neutron yields calculation,

$$\text{Total neutron yields} =$$

$$\int n_{\text{thermal,D}} n_{\text{fast,D}} \langle \sigma v \rangle (T_i, E_{\text{fast}}) \mathrm{d}V + \int n_{\text{thermal,D}} n_{\text{thermal,D}} \langle \sigma v \rangle (T_i) \mathrm{d}V + \int n_{\text{fast,D}} n_{\text{fast,D}} \langle \sigma v \rangle (E_{\text{fast}}) \mathrm{d}V,$$

where

$$n_{\text{thermal,D}} = n_e - \sum_j n_{\text{imp},j} Z_{\text{imp},j}$$

the scattering of the data points in figure 8(*a*) results from the uncertainty of the input data e.g. T_e, Z_{eff}, n_e, fast ion parameters such as $n_{\text{fast,D}}$ and E_{fast}, etc. The data points would be even more scattered if predicted T_i were used in the calculation. The neutron yield calculated with the T_i predicted by TRANSP-GLF23 (i.e. reference simulations) and by TRANSP-TGLF are compared against the measured neutron yields in figures 8(b) and 9, respectively. While the Pearson correlation coefficient of calculated neutron yields has significantly decreased by replacing the measured T_i with the T_i predicted by TRANSP- GLF23 i.e. from 0.942 in figure 8(*a*) to 0.825 in figure 8(*b*), the decrease is much smaller when replaced with T_i predicted by TRANSP-TGLF i.e. from 0.942 in figure 8(*a*) to 0.910 in figure 9. The higher accuracy of T_i predictions in TRANSP-TGLF enables much smaller impact on the neutron yields calculation.

5. Conclusion

Predictive simulations using TRANSP-GLF23 and TRANSP-TGLF of a large number of baseline H-mode discharges have been carried out to assess the present prediction capability for electron temperatures and ion temperatures in line with JET-DT preparation. A dependency of the T_e predictions on the collisionality regime is found in the TRANSP-GLF23 simulations i.e. under-prediction at low core ν^* and over-prediction at high core ν^*. The impact of core ν^* is less significant in the TRANSP-TGLF simulations where the trapped particle physics is modelled in a more complete way. As a result, the T_e prediction accuracy of TRANSP-TGLF is much improved compared to TRANSP-GLF23. The value of the core T_e predicted with GLF23/TGLF depends on the T_e boundary value, while neither GLF23 nor TGLF can model the transport in the ETB region. This means the radial position of the boundary value should be defined far enough into the core to exclude the ETB region in predictive simulations. It was also observed that the gradient of the predicted T_e profiles is not sensitive to the boundary T_e value (due to stiffness of the transport model). A uniform profile input of radiated power does not significantly change the results of TRANSP-GLF23/TGLF simulations for JET baseline H-mode discharges compared to the simulations with reconstructed radiation profile input as long as the total radiated power is correct. The *ExB* stabilisation model in GLF23/TGLF is a function of toroidal rotation, but in the 80 baseline H-mode discharges, TRANSP-GLF23 overpredicts the rotation significantly, so reliable rotation input and assumptions are necessary for JET-DT prediction. While the uncertainty in the T_i predictions with TRANSP-GLF23 significantly adds further uncertainty to neutron yields predictions, T_i predictions with TRANSP-TGLF have much better agreement with T_i measurements, thereby enabling better predictions of fusion power.

Acknowledgment

This work has been carried out within the framework of the EUROfusion Consortium and has received funding from the Euratom research and training programme 2014–2018

under grant agreement No 633053. The views and opinions expressed herein do not necessarily reflect those of the European Commission.

References

[1] Litaudon X. *et al* 2015 JET program for closing gaps to fusion energy *IEEE Trans. Plasma Sci.* **44** 1481–8

[2] Rimini F.G. *et al* 1999 Combined heating experiments in ELM-free H modes in JET *Nucl. Fusion* **39** 1591

[3] Strachan J.D. *et al* 1997 TFTR DT experiments *Plasma Phys. Control. Fusion* **39** B103–14

[4] Hawryluk R. 1979 An empirical approach to tokamak transport *Proc. of Physics of Plasmas Close to Thermonuclear Conditions, volume 1 (International School of Plasma Physics, Varenna, Italy, 27 August–8 September 1979)*

[5] Goldston R.J. *et al* 1981 New techniques for calculating heat and particle source rates due to neutral beam injection in axisymmetric tokamaks *J. Comput. Phys.* **43** 61–78

[6] Waltz R.E. *et al* 1992 Gyro-Landau fluid models for toroidal geometry *Phys. Plasmas* **4** 3138

[7] Waltz R.E. *et al* 1997 A gyro-Landau-fluid transport model *Phys. Plasmas* **4** 2482

[8] Staebler G.M. *et al* 2005 Gyro-Landau fluid equations for trapped and passing particles *Phys. Plasmas* **12** 102508

[9] Staebler G.M. *et al* 2007 A theory-based transport model with comprehensive physics *Phys. Plasmas* **14** 055909

[10] Pasqualotto R. *et al* 2004 High resolution Thomson scattering for joint European torus JET *Rev. Sci. Instrum.* **75** 3891

[11] Giroud C. 2008 Impact of calibration technique on measurement accuracy for the JET core charge exchange system *Rev. Sci. Instrum.* **79** 10F525

[12] Swinhoe M.T. *et al* 1984 Calculation and measurement of 235U and 238U fussion counter assembly detection efficiency *Nucl. Instrum. Methods Phys. Res.* **221** 460–5

[13] Syme D.B. *et al* 2014 Fusion yield mesasurements on JET and their calibration *Fusion Eng. Des.* **89** 2766–75

[14] Sips A.C.C. *et al* 2016 Assessment of the baseline scenario at q95~3 for ITER *Preprint: 2016 IAEA Fusion Energy Conf. (17–22 October 2016, Kyoto)* EX/P6-42 (https://conferences.iaea.org/indico/event/98/session/30/contribution/187)

[15] Frassinetti L. *et al* 2016 Dimensionless scalings of confinement, heat transport and pedestal stability in JET-ILW and comparison with JET-C *Plasma Phys. Control. Fusion* **59** 014014

[16] Kim H.-T. *et al* 2015 Comparative analysis of core heat transport of JET high density H-mode plasmas in carbon wall and ITER-like wall *Plasma Phys. Control. Fusion* **57** 065002

[17] Houlberg W.A. *et al* 1997 Bootstrap current and neoclassical transport in tokamaks of arbitrary collisionality and aspect ratio *Phys. Plasmas* **4** 3230

[18] Mast K.F. *et al* 1985 Bolometric diagnostics in JET *Rev. Sci. Instrum.* **56** 969–71

[19] Meister H. *et al* 2004 Z_{eff} from spectroscopic bremsstrahlung measurements at ASDEX upgrade and JET *Rev. Sci. Instrum.* **75** 4097–9

[20] Pankin A. *et al* 2004 The tokamak Monte Carlo fast ion module NUBEAM in the national transport code collaboration library *Comput. Phys. Commun.* **159** 157–84

[21] Brambilla M. 2002 'Quasi-local' wave equations in toroidal geometry with applications to fast wave propagation and absorption at high harmonics of the ion cyclotron frequency *Plasma Phys. Control. Fusion* **44** 2423–43

[22] Budny R. *et al* 2009 Progress testing TRANSP-TORIC simulations of ICRH in JET *36th EPS Conf. on Plasma Physics (Sofia, Bulgaria, 29 June–3 July 2009)* (www.euro-fusionscipub.org/wp-content/uploads/2014/11/EFDC090645.pdf)

[23] Stigler S.M. 1989 Francis Galton's account of the invention of correlation *Stat. Sci.* **4** 73–86

[24] Hammett G.W. *et al* 1990 Fluid moment models for landau damping with application to the ion-temperature-gradient instability *Phys. Rev. Lett.* **64** 25

[25] Kinsey J.E. *et al* 2008 The first transport code simulations using the trapped gyro-Landau-fluid model *Phys. Plasmas* **15** 055908

[26] PPPL TRANSP group http://w3.pppl.gov/transp/